

Supporting information for:

Dynamic permeability related to greisenization reactions in Sn-W ore deposits: Quantitative petrophysical and experimental evidence

Gaëtan Launay¹, Stanislas Sizaret¹, Laurent Guillou-Frottier¹, Colin Fauguerolles¹,
Rémi Champallier¹ and Eric Gloaguen¹

(1) Université d'Orléans/CNRS/ISTO/BRGM, UMR 7327, 1A rue de la Férollerie,
45071 Orléans, France

Electronic Supplementary Materials 1 (ESM 1)

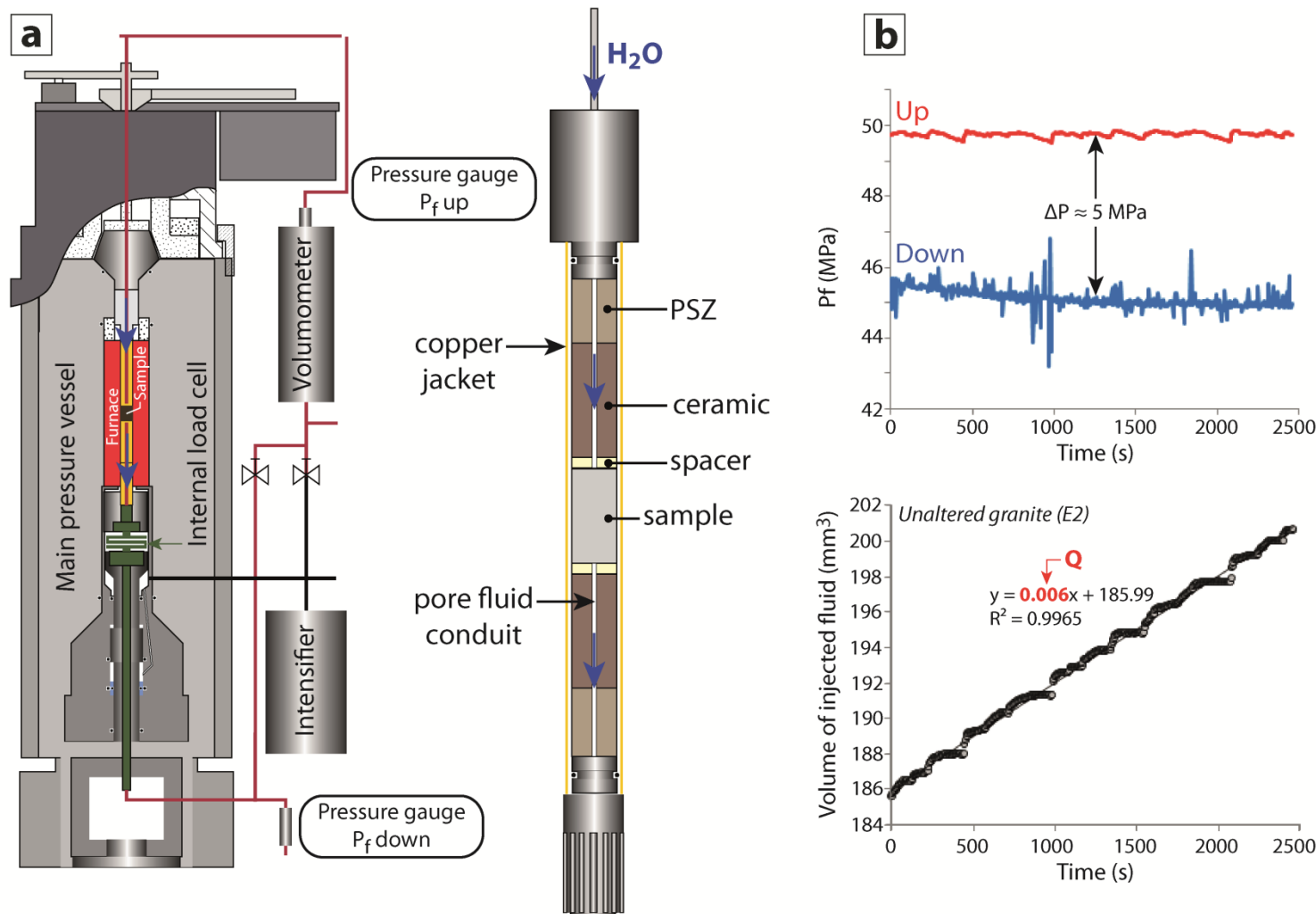


Figure 15: (a) Schematic representation of the Paterson apparatus and the pore fluid pressure system used for the permeability measurements (modified from Kushnir *et al.*, 2017). (b) Monitoring of the pressure fluid difference across the sample (ΔP) and the volume of fluid injected into the sample over the experiment time. The flow rate through the sample core was calculated from the linear regression shown in the diagram ($Q = 0.006$ mm³/s). From this flow rate and the pressure difference the permeability was estimated. This figure represents the measurement performed on the unaltered granite sample (E2).

Electronic Supplementary Materials 2 (ESM 2)

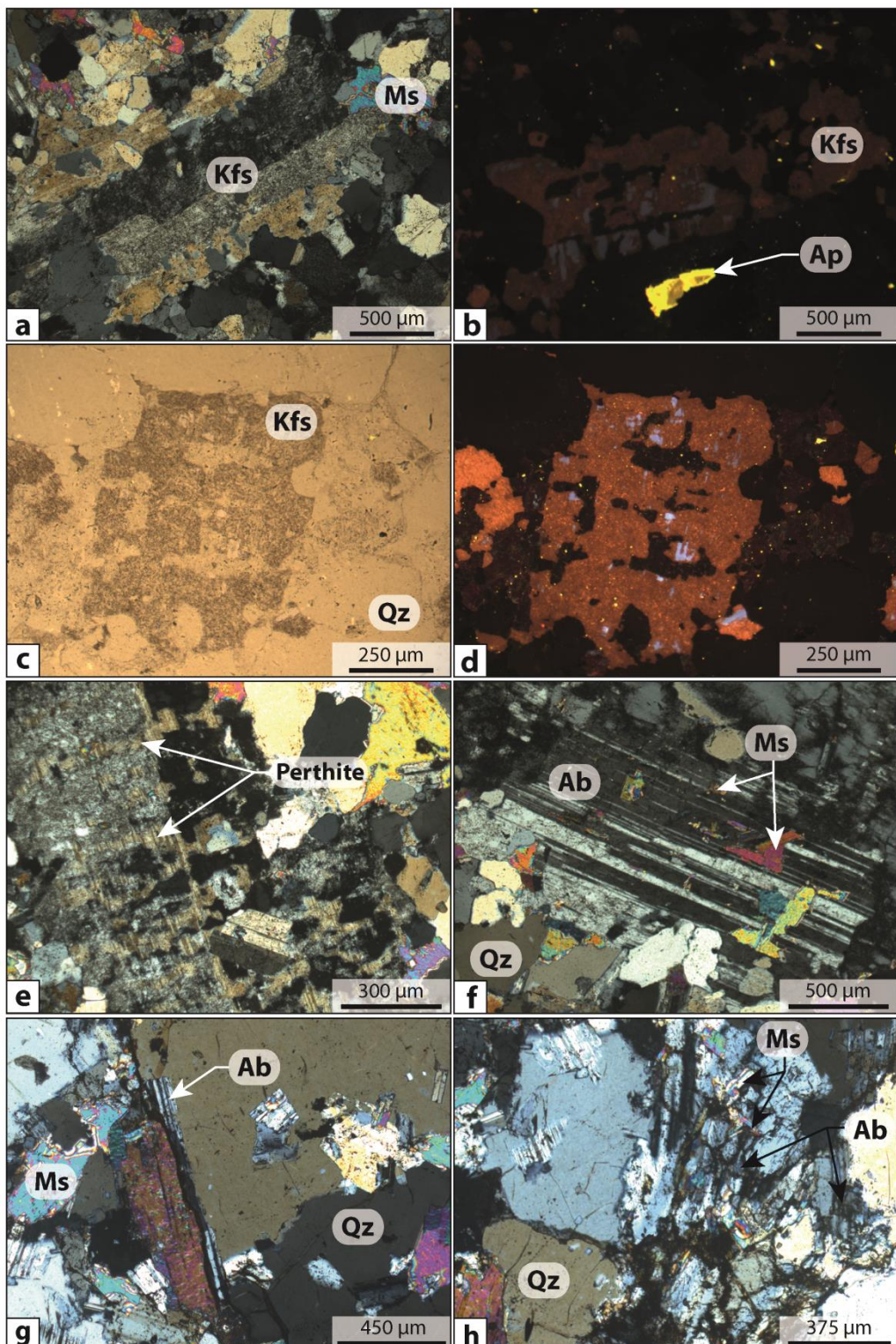


Figure 16 Photomicrographs of k-feldspars and albite composing the two-mica granite and the greisenized granite of Panasqueira. (a) to (c) Photomicrograph of matrix k-feldspars exhibiting replacement textures related to the early alkali metasomatism (a and c photomicrograph in transmitted light, b and d cathodoluminescence images). (e) Photomicrograph of k-feldspars exhibiting perthitic texture (transmitted polarized light). (f) Photomicrograph of albite in granite matrix (polarized transmitted light). (g) and (h) relics of albite partially replaced by muscovite (polarized transmitted light).

Electronic Supplementary Materials 3 (ESM 3)

wt%	Primary magmatic alkali feldspars (blue cathodoluminescence zones)										Metasomatized alkali feldspars (red cathodoluminescence zones)										
	SiO ₂	63.6	63.4	63.4	62.7	63.0	62.4	62.5	61.2	63.2	61.6	62.9	63.7	64.0	61.1	61.3	62.1	61.8	62.8	63.5	62.2
TiO ₂	0.0	0.0	0.0	0.0	0.0	0.1	0.0	0.0	0.0	0.0	0.0	0.0	0.0	0.0	0.0	0.0	0.0	0.0	0.0	0.1	0.1
Al ₂ O ₃	18.9	19.2	18.3	18.7	18.5	18.9	18.3	18.6	18.3	18.5	17.8	18.5	17.9	17.1	17.2	17.3	17.3	17.6	17.6	17.6	18.2
FeO	0.0	0.1	0.0	0.0	0.0	0.0	0.1	0.2	0.1	0.0	0.1	0.3	0.1	0.0	0.2	0.0	0.1	0.0	0.0	0.0	0.0
MnO	0.0	0.0	0.0	0.0	0.0	0.0	0.0	0.0	0.0	0.0	0.1	0.0	0.0	0.0	0.0	0.0	0.0	0.0	0.1	0.0	0.0
MgO	0.0	0.0	0.0	0.0	0.0	0.0	0.0	0.0	0.0	0.0	0.0	0.0	0.0	0.0	0.0	0.0	0.0	0.0	0.0	0.0	0.0
CaO	0.0	0.0	0.0	0.0	0.0	0.0	0.0	0.0	0.0	0.0	0.0	0.0	0.0	0.0	0.0	0.0	0.0	0.0	0.0	0.0	0.0
Na ₂ O	1.2	1.2	0.8	1.3	1.4	1.4	1.1	0.7	1.7	0.9	0.2	0.2	0.3	0.2	0.3	0.2	0.2	0.2	0.3	0.2	0.3
K ₂ O	15.1	15.1	16.1	15.0	14.7	14.6	15.2	15.3	13.6	15.8	16.1	16.5	16.5	16.5	16.9	16.6	16.6	16.5	16.7	15.7	
P ₂ O ₅	0.4	0.5	0.3	0.2	0.3	0.2	0.3	0.2	0.3	0.1	0.4	0.2	0.1	0.1	0.1	0.0	0.0	0.1	0.2	0.2	
Total	99.1	99.6	99.0	98.1	97.9	97.6	97.5	96.3	97.0	97	97.6	99.4	98.8	95.2	95.9	96.4	96.1	97.3	98.1	96.8	
Ab (%)	11	11	7	12	12	13	10	7	16	8	2	2	3	2	2	2	2	2	2	3	
Or (%)	89	89	93	88	88	87	90	93	84	92	98	98	97	98	98	98	98	98	98	97	
An (%)	0	0	0	0	0	0	0	0	0	0	0	0	0	0	0	0	0	0	0	0	

Table 3 EPMA analyses of alkali feldspars composing the least altered two-mica granite of Panasqueira.

wt%	Plagioclase from least altered two-mica granite									
SiO₂	65.4	66.6	68.0	68.4	68.2	68.7	68.9	68.5	68.0	69.2
TiO₂	0.0	0.0	0.0	0.0	0.0	0.0	0.0	0.0	0.0	0.0
Al₂O₃	18.6	21.4	19.2	19.2	19.1	19.3	19.4	19.5	19.3	18.9
FeO	0.0	0.1	0.0	0.0	0.0	0.0	0.0	0.0	0.0	0.1
MnO	0.0	0.0	0.0	0.0	0.0	0.0	0.0	0.0	0.0	0.0
MgO	0.0	0.0	0.0	0.0	0.0	0.0	0.0	0.0	0.0	0.0
CaO	0.6	0.2	0.1	0.0	0.0	0.0	0.0	0.0	0.3	0.0
Na₂O	11.5	9.8	11.4	11.2	11.2	11.1	11.2	9.9	10.7	10.3
K₂O	0.1	0.9	0.1	0.1	0.1	0.2	0.1	0.1	0.2	0.0
P₂O₅	0.2	0.2	0.0	0.0	0.0	0.1	0.1	0.0	0.0	0.0
Total	96.4	99.1	98.9	99.0	98.7	99.4	99.8	98	98.5	98.6
Ab (%)	96	93	99	99	99	99	99	99	97	1
Or (%)	1	6	1	1	1	1	1	1	1	0
An (%)	3	1	0	0	0	0	0	0	3	0

Table 4 EPMA analyses of plagioclase composing the least altered two-mica granite of Panasqueira.

Electronic Supplementary Materials 4 (ESM 4)

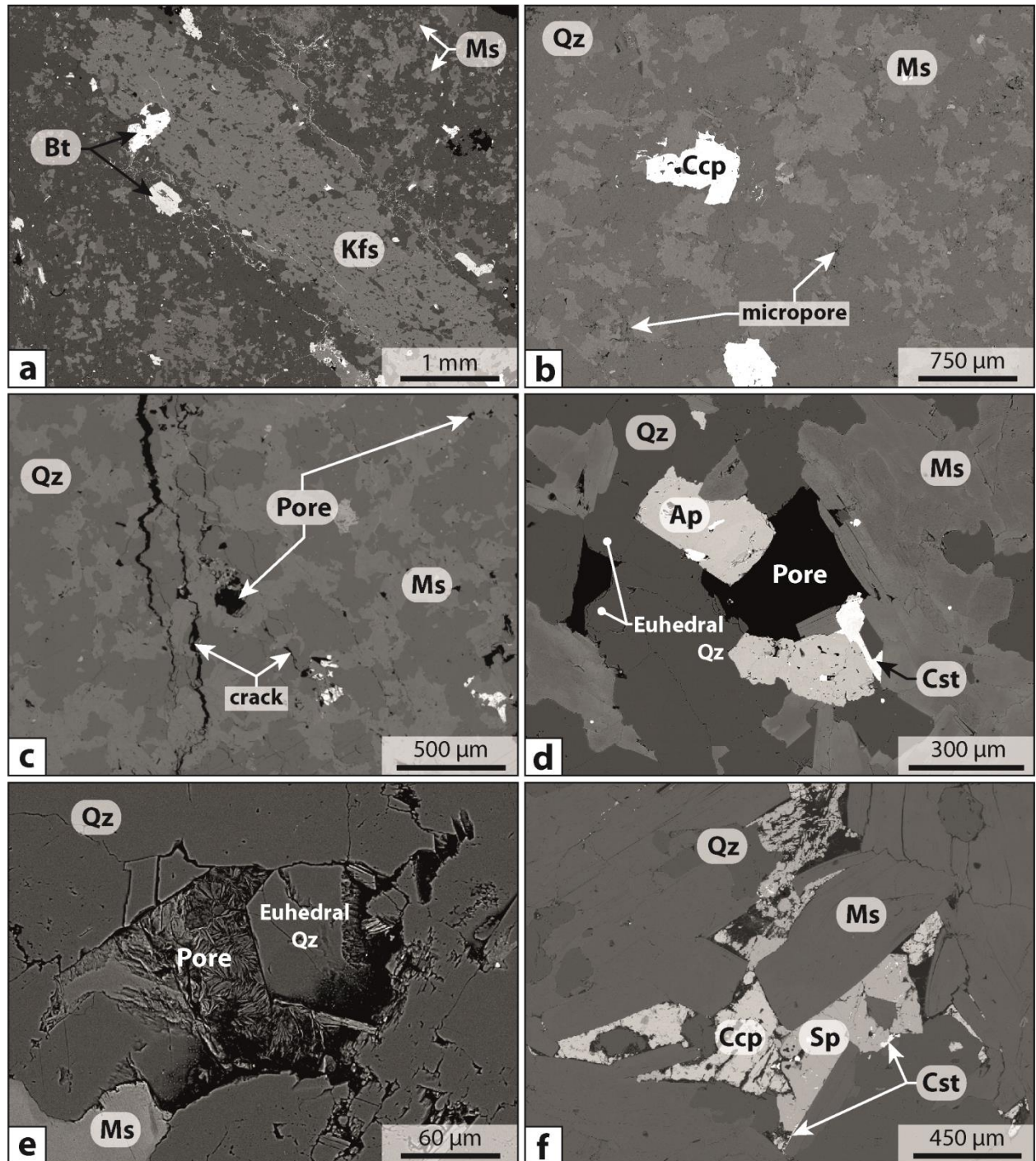


Figure 17: More SEM-BSE images showing the microtextural characteristics of greisenized granite and greisen of Panasqueira. (a) Section of k-feldspars partially altered into muscovite during greisenization. Note the presence of micropores and microcracks, which were completely infilled by sulfide minerals (pyrite and chalcopyrite) during the late sulfide stage. (b) Section of greisenized granite displaying microporous texture. (c) Section of quartz-muscovite greisen displaying large pores, cracks and microcracks. (d) and (e) zoom on greisen porosity, in which apatite, cassiterite and euhedral quartz have crystallized. (f) Greisen porosity completely infilled by sphalerite and chalcopyrite.

Electronic Supplementary Materials 5 (ESM 5)

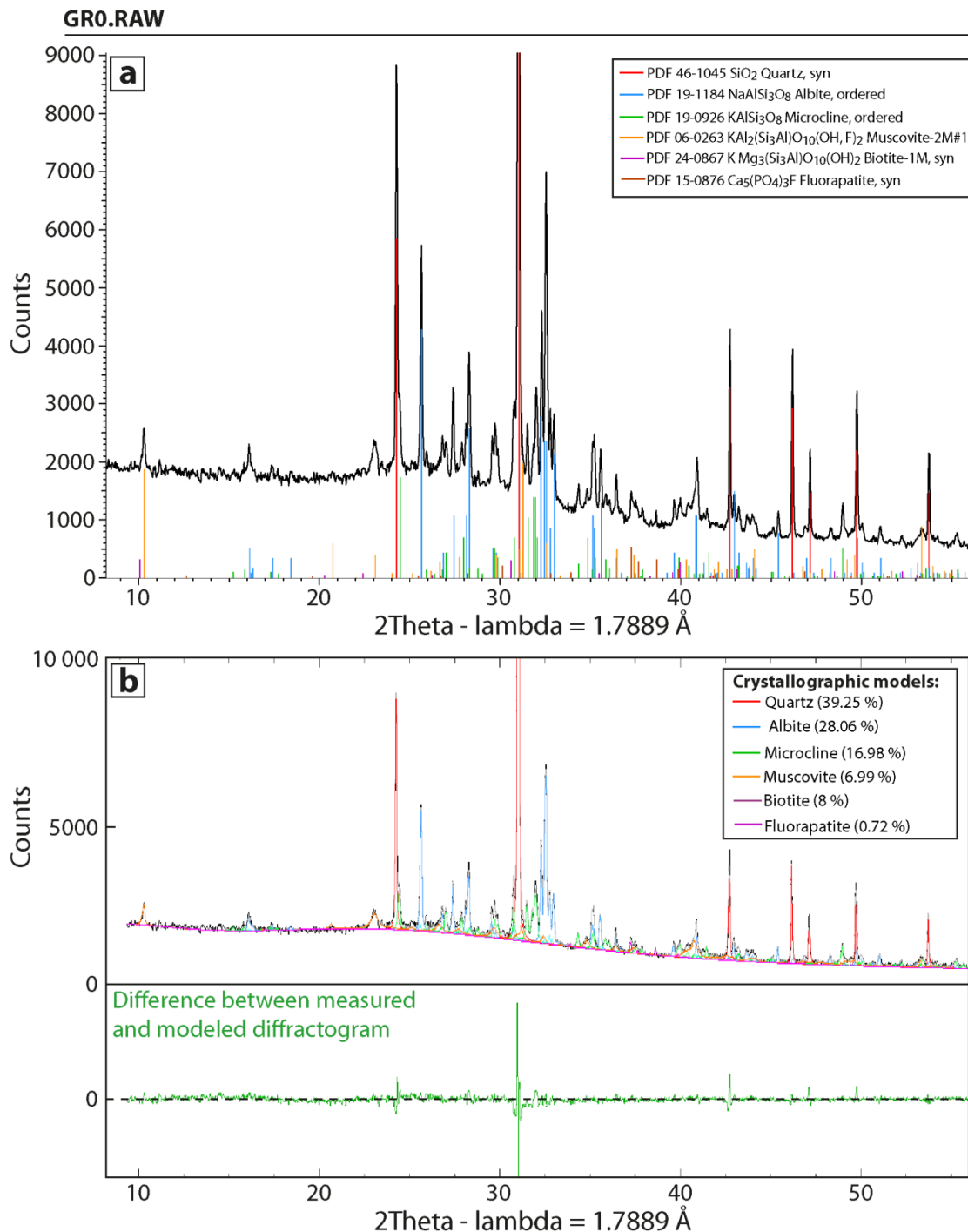


Figure 18: (a) X-Ray Diffractogram (XRD) obtained from powder of the unaltered Panasqueira granite. The XRD acquisitions were performed on an INEL diffractometer using a curve position-sensitive detector (CPS-120). The mineral identification was realized using the mineral database of Profex. (b) Results of mineral quantification obtained from Profex-Rietveld method. This method consists of simulating a diffractogram from crystallographic models and adjusts the mineral abundances to obtain a simulated diffractogram as close as possible to the measured diffractogram. The mineral abundances are indicated for each minerals and the difference between the measured and modeled diffractogram are displayed below the spectra.

Electronic Supplementary Materials 6 (ESM 6)

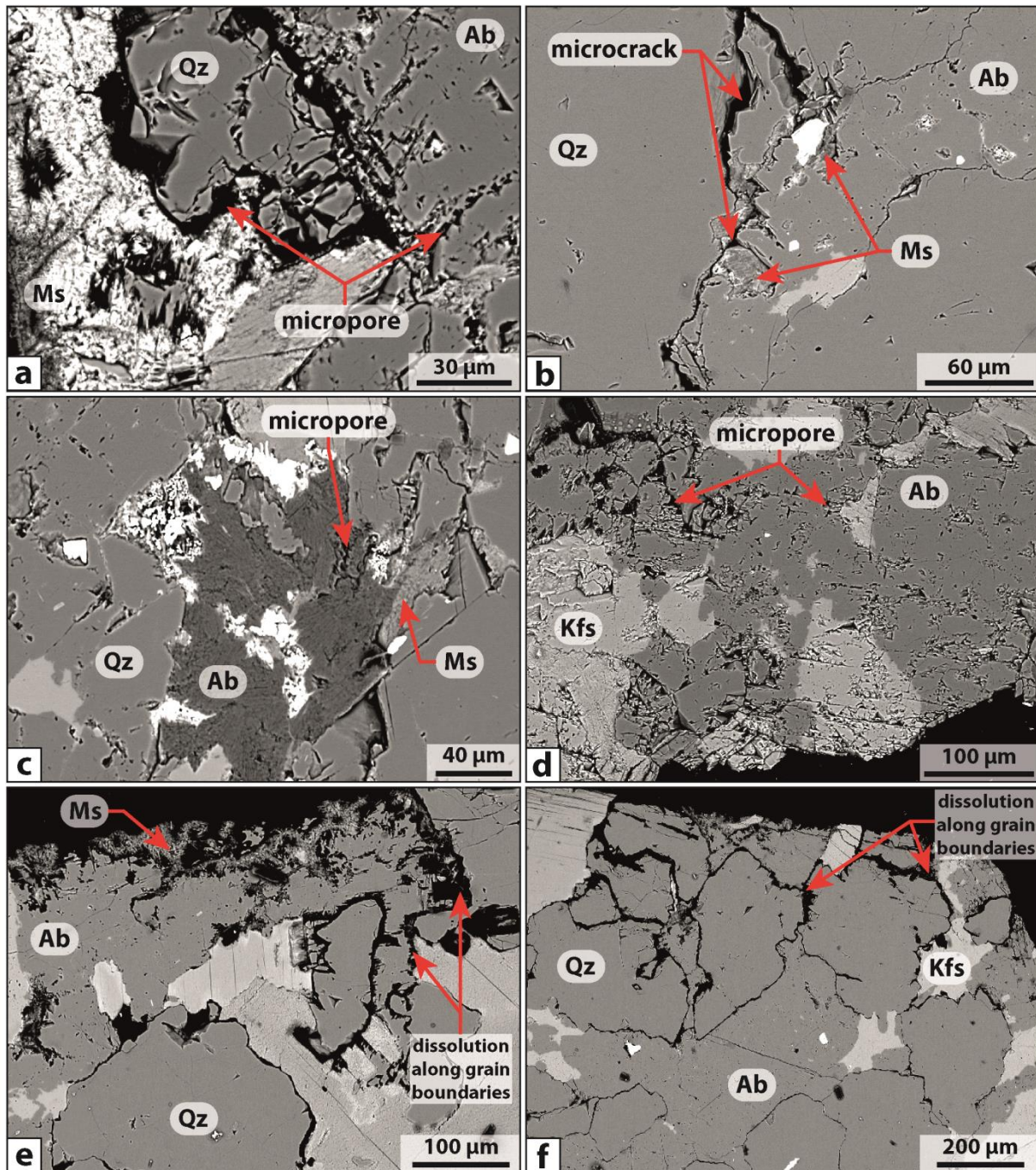


Figure 19: SEM-BSE images showing the alteration products and textures produced during the greisenization experiment. (a to c) Grains of albite partially replaced by muscovite along the grain boundaries and along microcracks. (d) Micropores developed in grains of albite and k-feldspar emphasizing the partial dissolution of feldspars during the greisenization. (e to f) Dissolution of albite along the grain boundaries and precipitation of muscovite along the edge of the granite core. All of these textures highlight that replacement reactions related to greisenization generate new pathways in greisenized facies.

Electronic Supplementary Materials 7 (ESM 7)

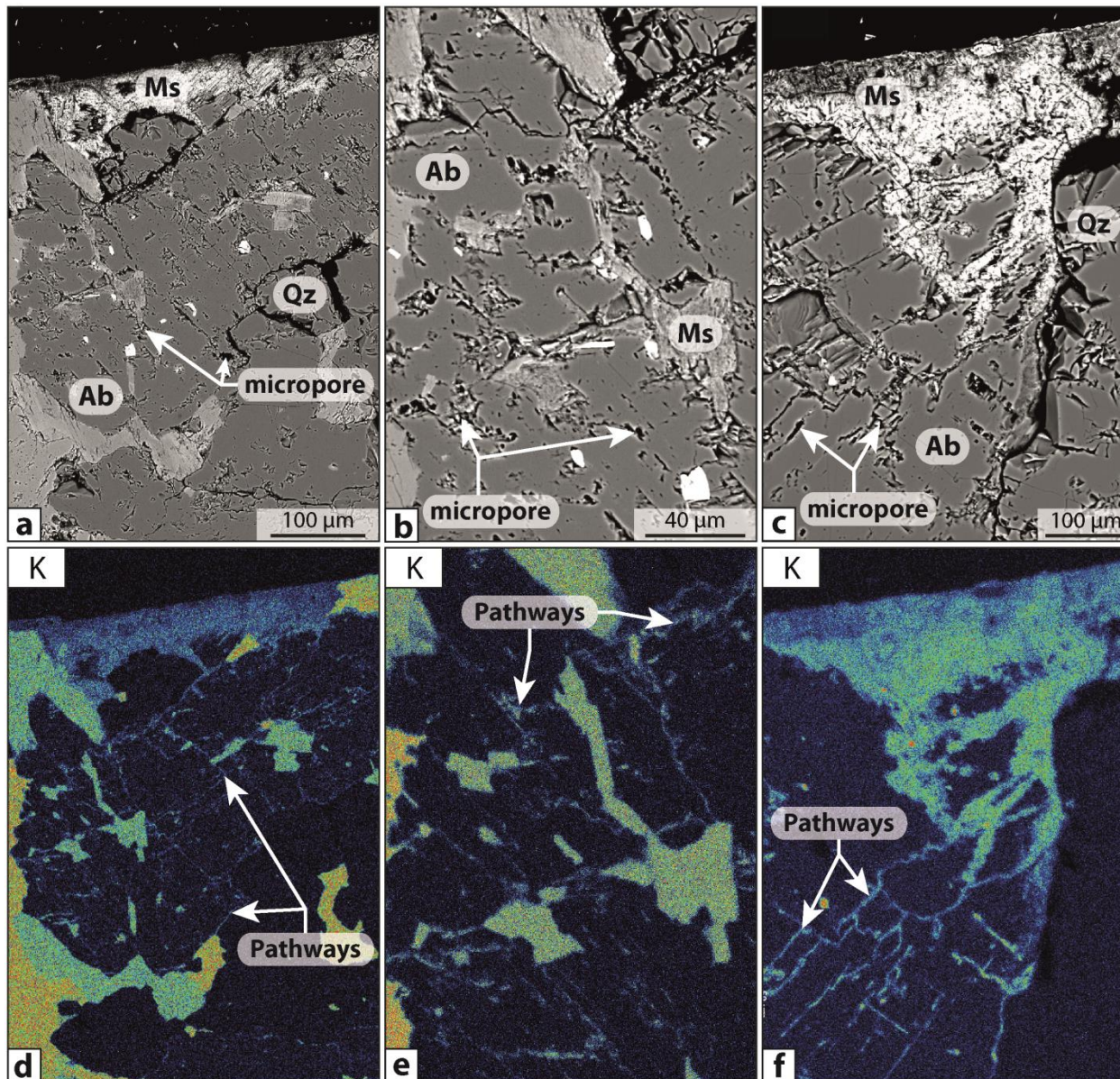


Figure 20: (a to c) SEM-BSE images and (d to f) geochemical mapping of K showing the pathways along which fluids have preferentially flowed and altered albite into muscovite during the greisenization experiment. The transformation of albite into muscovite occurred mainly along the grain boundaries and along the cleavage planes of albite. Note the presence of micropores in partially altered section of albite.

Electronic Supplementary Materials 8 (ESM 8)

	SiO ₂	Al ₂ O ₃	Fe ₂ O ₃	CaO	MgO	Na ₂ O	K ₂ O	TiO ₂	MnO	P ₂ O ₅	LOI	Total
Granite												
D3	72.3	13.4	2.33	0.56	0.25	3.72	3.89	0.19	0.05	0.43	1.03	98.15
D1	72.7	13.65	1.91	0.66	0.27	3.41	4.21	0.2	0.05	0.44	0.96	98.46
D4	75.1	14	2.18	0.56	0.26	3.12	4.1	0.19	0.06	0.38	0.89	100.84
D2	73.2	13.9	2.19	0.64	0.31	3.32	4.35	0.22	0.05	0.4	1	99.58
E2	73.9	13.5	2.1	0.53	0.26	3.82	3.97	0.19	0.05	0.39	1.12	99.83
Greisenized granite												
C1	73.5	14.25	2.57	0.53	0.19	3	3.67	0.14	0.07	0.43	1.83	100.18
O4	78.3	12	1.34	0.24	0.02	4.06	1.86	0.01	0.05	0.2	0.94	99.02
P3D	80.7	12.05	1.51	0.23	0.02	3.66	2.04	0.01	0.05	0.21	0.93	101.41
P3E	74.9	14.5	1.92	0.71	0.04	3.62	2.85	0.01	0.09	0.58	1.31	100.53
P3C	74.1	14.6	2.46	0.56	0.22	2.72	3.56	0.12	0.07	0.45	1.76	100.62
O3	74.4	14	2.06	0.85	0.04	3.74	2.6	0.01	0.12	0.71	1.14	99.67
O1	73.1	14.9	2.5	0.55	0.23	2.79	3.48	0.11	0.06	0.45	1.88	100.05
O5	76.6	12.55	2.36	0.27	0.05	1.47	3.55	0.02	0.05	0.25	1.21	98.38
P4-2	79.4	10.55	2.69	0.3	0.04	0.22	3.52	0.02	0.06	0.25	1.25	98.3
P4-3	78.7	11.95	1.92	0.3	0.05	1.73	3.13	0.02	0.05	0.27	1.31	99.43
P4-A	77.2	12.55	2.38	0.27	0.07	1.47	3.29	0.02	0.05	0.23	1.38	98.91
Greisen												
B2	71.6	16.55	3.07	0.48	0.23	0.21	5.46	0.12	0.07	0.39	2.45	100.63
B1	70.1	16	2.97	0.49	0.23	0.2	5.1	0.13	0.07	0.45	2.37	98.1
P57-A	72.1	16.65	3.08	0.47	0.25	0.22	5.61	0.13	0.07	0.38	2.4	101.36

Table 5 Major elements composition (in wt%) for granite, greisenized granite and greisen used to establish the chemical alteration index (AI).

	Least altered granite						Less altered	Intermediate	Most altered	
(wt%)	D2	D3	D5-A	D1	D5-B	Average	SD	C1	C2-A	B1
SiO ₂	73.2	72.3	73.9	72.7	73.5	73.12	0.63	73.5	74.6	70.1
Al ₂ O ₃	13.9	13.40	13.5	13.65	13.45	13.58	0.20	14.25	14.7	16
Fe ₂ O ₃	2.19	2.33	2.1	1.91	2.12	2.13	0.15	2.57	2.54	2.97
CaO	0.64	0.56	0.53	0.66	0.51	0.58	0.07	0.53	0.56	0.49
MgO	0.31	0.25	0.26	0.27	0.25	0.27	0.02	0.19	0.23	0.23
MnO	0.05	0.05	0.05	0.05	0.05	0.05	0.00	0.06	0.06	0.06
Na ₂ O	3.32	3.72	3.82	3.41	3.7	3.59	0.22	3	2.79	0.2
K ₂ O	4.35	3.89	3.97	4.21	3.65	4.01	0.27	3.67	3.34	5.1
TiO ₂	0.22	0.19	0.19	0.2	0.18	0.19	0.02	0.14	0.12	0.13
P ₂ O ₅	0.4	0.43	0.39	0.44	0.35	0.40	0.04	0.43	0.45	0.45
LOI	1	1.03	1.12	0.96	1.28	1.08	0.13	1.83	1.84	2.37
Total	99.58	98.15	99.83	98.46	99.04	99.01		100.18	101.23	98.1
(ppm)										
Ba	66.9	53.7	55.6	59.1	54.6	57.98	5.39	27.3	29	27.1
Eu	0.23	0.16	0.22	0.22	0.19	0.204	0.03	0.1	0.11	0.1
Sr	23.1	22.4	23.1	23.9	23.2	23.14	0.53	15.5	13.1	10.2
Cs	21.5	17.45	17.8	18.9	17.95	18.72	1.64	35.8	51.1	42.1
Li	340	300	300	300	310	310	17.32	560	590	600
Sn	35	28	27	27	24	28.2	4.09	57	131	138
W	14	10	9	9	9	10.2	2.17	28	33	36
Zr	86	89	79	82	78	82.8	4.66	42	40	31
As	8	5	6	5	5	5.8	1.30	220	220	261
Cu	3	1	2	1	1	1.6	0.89	97	99	102
Zn	78	59	61	65	64	65.4	7.44	318	326	294
Rb	494	457	456	477	452	467.2	17.85	737	907	1065

Table 6 Major and trace elements composition of granite and sample representative of different degree of greisenization used to realize the isocon diagram